Bioinspired Active Electrosensing System for Microscopic Robots

Janet Z Wang, Princeton University Department of Electrical and Computer Engineering, *SUNFEST Fellow*
Professor Marc Miskin, University of Pennsylvania Department of Electrical and Systems Engineering

***Abstract*—Microscopic robots enable us to engage with the microscopic world in an exciting new way. A sensing mechanism must be developed for microrobots to sense and navigate their aqueous environment. We propose a sensing mechanism inspired by the biological sensing modality employed by some species of freshwater fish, active electrosensing, but at the microscale. We fabricated titanium-platinum bilayer microelectrode arrays to investigate sourcing and measuring AC signals in a conductive solution with no occlusions, built a probing setup to make electrical contact with the microelectrodes, and developed an experimental plan to quantify the effect of factors such as occlusion location and size on differential measured voltage signals in solution. This work serves as a step towards demonstrating the viability of developing an active electrosensing system for robots at the microscale.**

I. Introduction

With a broad range of potential applications in medicine and industry, microscopic robots promise the opportunity to engage with the microscopic world in an exciting new way. Our group has developed walking microrobots based on voltage-controlled electrochemical actuators that are compatible with semiconductor processing and can be integrated with CMOS electronics to move autonomously powered solely by incident daylight [4, 6]. Current research efforts aim to incorporate on-board electronic circuits including voltmeters, thermometers, solar cells, and even a microcontroller, as well as improve actuator performance in order to achieve more advanced functionality.

In the quest to develop fully autonomous microrobots that are capable of complex programmable tasks, a sensing mechanism must be developed for the microrobots to sense and navigate their aqueous environments. Since existing underwater sensing technologies in robotics based on light and sound cannot be easily appropriated at the microscale, we propose a sensing mechanism at the microscale inspired by the biological sensing modality of active electrolocation employed by some species of freshwater fish.

Previous work has demonstrated an active electrosensing system for macroscale underwater robots to avoid objects and detect the sizes of objects; however, we are interested in active electrosensing on a much smaller scale for microrobots.

In this paper, we aimed to demonstrate the viability of developing an active electrosensing system for robots at the microscale. To accomplish this, we fabricated titanium-platinum bilayer microelectrode arrays to investigate sourcing and measuring AC signals in a conductive solution with no occlusions. We also built a prototype probing station to make electrical contact with the microelectrodes. Lastly, we developed an experimental plan to quantify the effect of factors such as the location and size of the occlusion on the measured voltage signals in the solution.

II. Background

A. Microscopic robots

Half a century of CMOS technology scaling as observed by Moore's law has resulted in exciting opportunities for microscopic robotics. Advancements in electronic, magnetic, and optical technologies have enabled a new era for microtechnology and the development of microrobots employing a variety of materials, fabrication technologies, and control methods [2]. Microrobots may be smaller than 100μm in size, which is smaller than the resolution limit of human vision.

Prior work has has prototyped sub-100μm walking robots using lithographic fabrication-and-release protocols that allow for the production of over one million robots on one 4-inch silicon wafer. These walking microrobots are enabled by the development of microscale voltage-controllable surface electrochemical actuators that can operate at low voltages and low power [6]. Additionally, autonomous microscopic robots that can be powered by sunlight are being developed by researchers by integrating foundry-produced 180nm CMOS electronics with optical input/output and surface electrochemical actuators [4].

Microscopic robots have potential applications in adaptable sensors, neural interfacing, and regenerative medicine. For example, microrobots could navigate hard-to-reach sites in the human body and noninvasively perform specific tasks. With a focus in the development of microrobots that can operate robustly in complex physiological environments, microrobots have the potential to transform medicine and healthcare [3].

With new developments in silicon electronics and intelligent control algorithms in robotics, microscopic robotics is an exciting, rapidly developing research field.

B. Active electrosensing

Some fish, such as sharks and catfish, engage in passive electrolocation, in which they are able to detect electrical signal changes in their environment. Others, such as some species of freshwater fresh in Africa and South America, are active electrolocators—they not only can *sense* electric fields but also can *emit* them to detect objects in their environment [5].

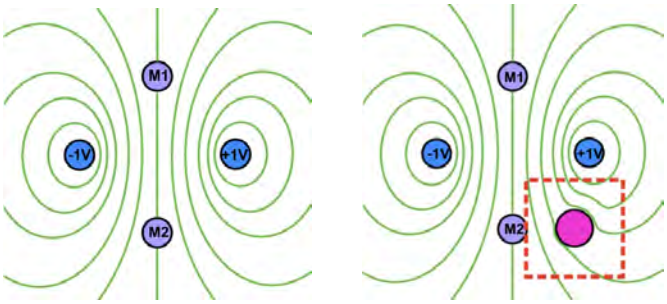

(a) (b)

Fig. 1. Example of active electrosensing in 2D. The two blue circles represent the source electrodes as electric dipoles, and the two purple circles represent the measurement electrodes that measure the voltage signal at their locations. All electrodes are equidistant from the center. The green lines are equipotential contours. 1a shows the scenario with no occlusion, in which we measure a differential potential between M1 and M2 of zero. 1b shows the scenario with an occlusion (represented by the pink circle). The red box highlights the perturbation to the electric field due to the occlusion. In this scenario, we measure a nonzero differential potential between M1 and M2.

The principle of biological active electrolocation is that objects with an impedance that differs from their aqueous environment distort the electric field generated by the fish, and sensors on the fish's body detect these field distortions [7].

Biological active electrosensing has inspired the development of a new sensing modality for robots. At the macroscale, in addition to echolocation (sensing using sound perturbations), robotic active electrosensing may be used for detecting objects in darkness, where vision proves to be ineffective. Researchers developed a robotic sensing system for underwater target localization at the macroscale with a 46cm long robot, focusing on designing and testing active motion and statistical learning algorithms to localize spherical and ellipsoidal objects [1].

Figure 1 shows an example of the concept of active electrosensing in a system.

III. Materials and Methods

The microelectrode arrays (Ti and Pt bilayer patterned on a glass wafer substrate) were fabricated using photolithography, physical vapor deposition, and lift-off processes in a micro-/nanofabrication facility. Figure 2 shows images of the fabricated microelectrode arrays. See Appendix A for the detailed fabrication procedure.

In order to source and measure voltage signals on our fabricated microelectrodes, we built a probe station to make electrical contact with the square electrodes with a side length of 70µm, the thickness of a human hair. The electrodes fabricated on the glass slide were placed at the bottom of a glass petri dish filled with phosphate buffered saline (PBS) 1X or deionized water to vary solution conductivity. Four platinum/iridium probes with a tip diameter of 2µm and 25:1 taper (two for sourcing and two for measuring) were mounted to four Signatone SP-100 Precision In-Line Micropositioners. Probes were lowered into the solution and carefully placed in electrical contact with electrode pads using the micropositioners to move probes with micrometer precision and Zeiss Stereo Microscope to view the probes and electrodes.

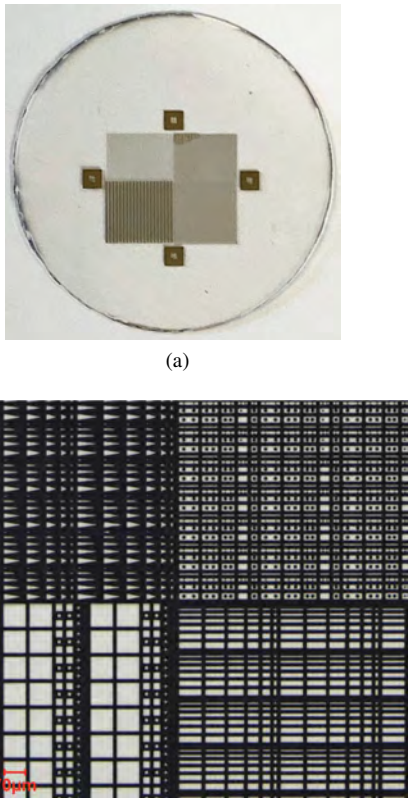

(a) (b)

Fig. 2. Microelectrode array fabrication results. 2a shows an image of the electrodes on a 1-inch glass wafer substrate. 2b shows a micrograph of the center of the wafer pattern with the square electrodes tested in this paper shown in the bottom left corner. Micrograph by Lucas Hanson.

Figure 1 shows the concept of active electrosensing but with the sourced voltages as DC electric dipoles. In our system, however, our source and measurement electrodes are platinum and thus a sinusoidal AC voltage signal must be sourced because platinum electrodes act as capacitors in our voltage range of 100mV. When no occlusions are present, the differential voltage of M1 and M2 is zero. When an occlusion is present, the occlusion disrupts the electric field and result in a nonzero differential M1 and M2 voltage measurement. Sinusoidal AC voltage with an amplitude of 100mV and frequency of 500Hz was sourced (S- and S+) and two voltage signals were measured (M1 and M2) using the PicoScope 5000D Series oscilloscope and corresponding PicoScope 6 software. Probes were connected to the PicoScope via BNC connections. Figure 3b shows the prototype probing setup and a magnified image of the four probe tips contacting the platinum microelectrode pads in solution.

Our main experiment involved sweeping the location of the measurement electrodes and measuring the peak-peak voltages of the signal in solution. We also varied the experimental parameters of solution conductivity, source frequency, source voltage amplitude, and probe submersion depth to define their effect on the measured voltage signal. We were primarily concerned with the differential peak-peak voltage between the

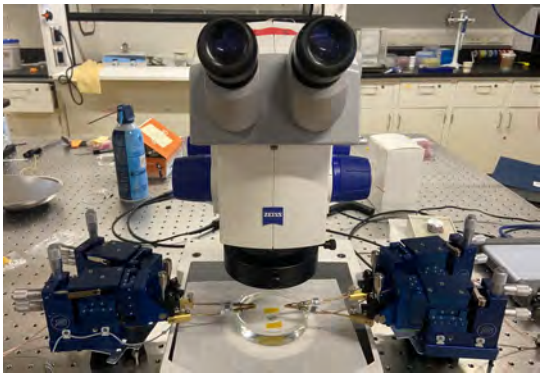

(a)

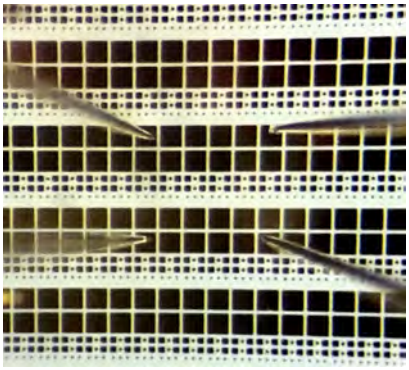

(b)

Fig. 3. Probing microelectrodes. 3a shows the probing station setup with the stereo microscope and four micromanipulators each with a platinum/iridium probe. The function generator and oscilloscope are not shown. 3b is an image of the four probe tips contacting the platinum electrode pads as seen in the Zeiss Stereo Microscope.

M1 and M2 electrodes: V_M.

To test the concept of active electrosensing at the microscale, an occlusion between the electrodes must be introduced. A photomask defining four experiments varying occlusion and electrode pad parameters was designed and an experimental plan to fabricate Ti-Pt bilayer microelectrode arrays with occlusions of SU-8 photoresist was developed. Photomasks used in photolithography were designed in LayoutEditor.

Figure 4 shows the photomask design for future occlusion experiments. Windows around the array of experiments in the second photomask were added to make course aligning easier. Alignment pads provided by the Quattrone Nanofabrication Facility were used to align the two layers (metal and SU-8) during photolithography. The first photomask defines the locations and sizes of the source and measurement electrodes as well as the text labels. The second mask defines the locations and sizes of the occlusion in each experiment.

IV. Results and Discussion

We did not observe any significant difference in the measured differential voltage signal when the distance of measurement electrode M2 from source electrode S+ was increased, as shown in Figure 5. The average peak-peak of the measured voltage signal should theoretically decrease as the measurement electrode is moved farther away from the source

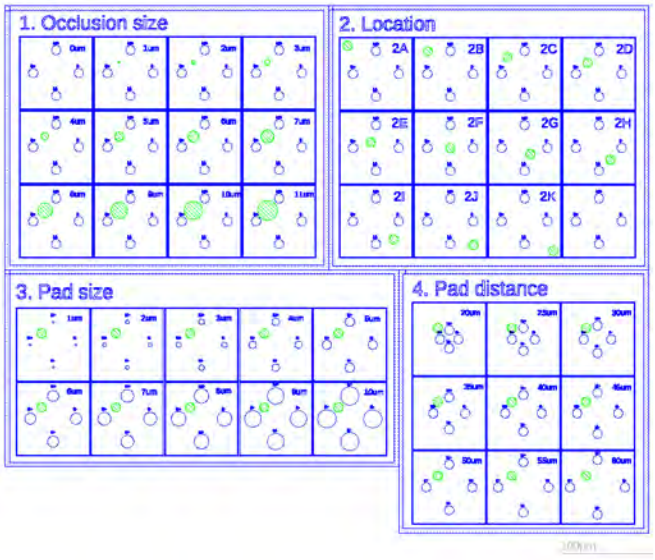

(a)

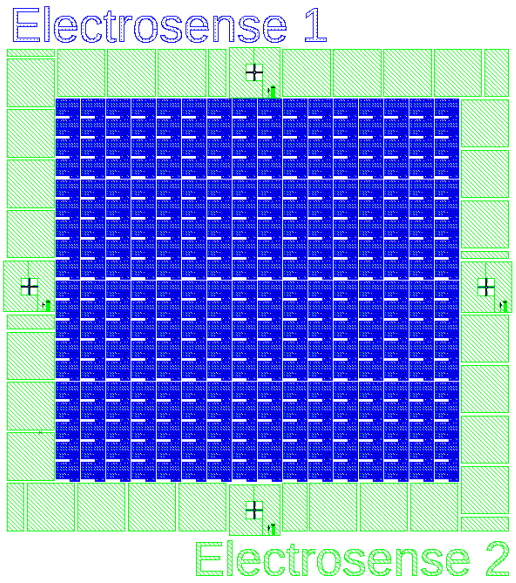

(b)

Fig. 4. Experiments with occlusions defined on photomask. 4a shows one block with all four experiments. 4b shows the full mask design with $16 \times 19 = 304$ blocks. Ti and Pt depositions (first photomask) are shown in blue. SU-8 (second photomask) is shown in green.

electrode due to the resistivity of the solution. This result shows that further experimentation and probing setup revision is needed to determine the viability of active electrosensing at the microscale with no occlusions.

We verified that the measured voltage signal differed depending on whether the measurement probe was in contact or not in contact with the electrode, as shown in Figure 6 in the change in V_M at a z-distance above pad of 0mm (probe in contact with electrode pad) and 1mm (probe not in contact with electrode pad).

We also found that the measured differential peak-peak voltage signal increases as the platinum/iridium probe is lifted above the electrode pad. This shows the strong dependence of

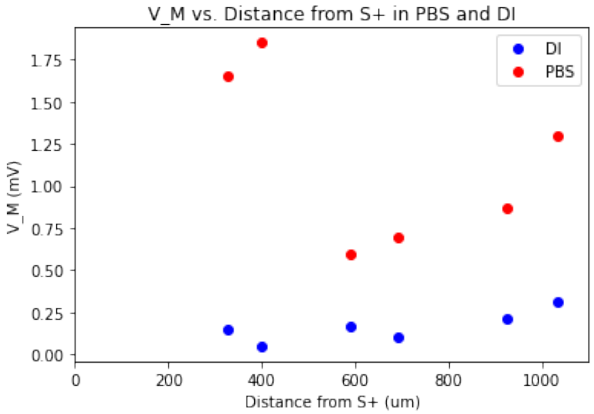

Fig. 5. No observed difference in measured differential signal as measurement probe moves farther away from source probe. V_M is the differential peak-peak voltage between M1 and M2.

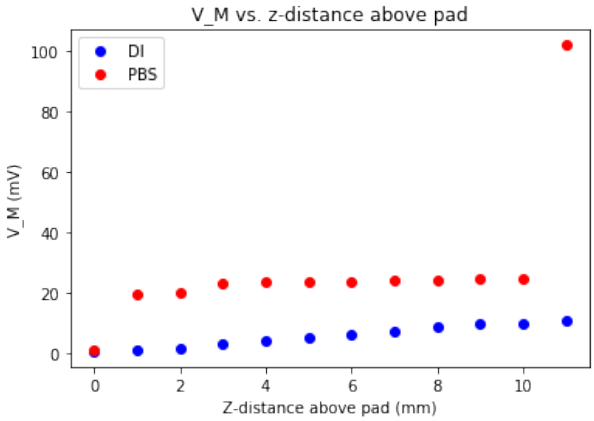

Fig. 6. Dependence of measured differential signal on measurement probe submersion depth. A z-distance above pad of 0 means the measurement probe is in contact with the electrode pad. A z-distance of 11mm is when the probe tip is in air and not in the solution.

the measured voltage signal on the properties of the probe. The measured differential voltage peak-peak signal has a higher dependency on probe submersion depth in DI water compared to PBS.

Using this probing setup, we sourced and measured AC signals by making electrical contact to the four microelectrodes with the probes. We identified a rough dependence in the measured differential voltage as we varied the location of the measurement probe but were unable to measure a trend above the noise floor of the system. To investigate further, we varied experimental parameters and identified the dependence of the measured voltage signal on solution conductivity, source frequency, source voltage amplitude, and probe submersion depth.

From our experiments, we determined that our prototype probing setup is sensitive to the properties of the probes, and the measured voltage signal is dominated by the impedance of the probes rather than the microelectrodes we aimed to probe. The probing setup must be improved to isolate the desired measured voltage signal for analysis in future experiments.

V. Conclusion

In summary, we fabricated microelectrode arrays and built a prototype probing station to test sourcing and measuring voltage signals in solution, pinpointing the dominance of probe impedance on measured voltage signals, as a first step towards demonstrating the viability of developing an active electrosensing system for microscopic robots. Future work involves revising the probing setup and experimental design to reduce the voltage dependence on the probe properties. For example, we may consider electrodes of different sizes, shapes, and materials. Additionally, we may implement more robust signal processing by using a differential amplifier, for example, to increase the signal-to-noise ratio and hopefully be able to measure a change in measured voltage signal with varied measurement probe location.

We aim to verify proper differential voltage signal measurement in solution with no occlusions, as well as quantify the effect of occlusions on the measured electric field in solution by making the photomasks described in Section III and fabricating the Ti-Pt microelectrode arrays including SU-8 occlusions.

Appendix A
Microfabrication Process

Microelectrode arrays consisted of a bilayer of Ti and Pt patterned onto a circular glass wafer substrate with a 1-inch diameter. The microelectrode arrays were fabricated in a micro-/nanofabrication facility using standard photolithography and lift-off protocol. Fabrication process was done in parallel for 8 to 14 glass slides.

1) Starting with a 500µm-thick glass slide, rinse in acetone and isopropyl alcohol with sonication for 20min at 60°C. Blow dry with nitrogen gas.
2) Run the O_2 plasma descum recipe for 10min on the Oxford 80 Plus Reactive Ion Etcher.
3) Spincoat LOR3A lift-off photoresist at 500rpm for 5s and 3000rpm for 40s, and then bake at 150°C for 5min on a hotplate.
4) Spincoat S1813 positive photoresist at 500rpm for 5s and 3000rpm for 40s, and then bake at 115°C for 1min 30s on a hotplate.
5) Load first photomask into SUSS MicroTec MA6 Gen3 Mask Aligner mask chuck and load glass slide into 1in wafer chuck. Expose at dose of 155J/cm^2.
6) Develop in AZ 300 MIF developer with agitation for 40s, rinse in deionized water, and blow dry with nitrogen gas. Verify proper development on Zeiss Axio Imager M2m Microscope.
7) Deposit 20nm of Ti (450°C for 120s) followed by 40nm of Pt (450°C for 180s) using the Denton Explorer14 Magnetron Sputterer.
8) Lift off in remover PG at 60°C for 40min with sonication. Rinse in deionized water and blow dry with nitrogren gas. Verify proper lift-off on Zeiss Axio Imager M2m Microscope.

A schematic summarizing the microelectrode array fabrication process is shown in Figure 7. Figure 8 shows the full

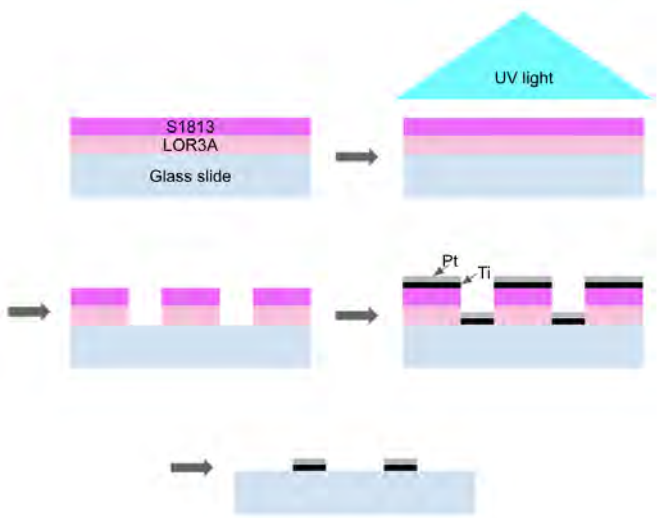

Fig. 7. Microfabrication process summary (not drawn to scale). 1. Spin photoresist, 2. UV expose with photomask, 3. Develop, 4. Deposit metal, 5. Lift-off.

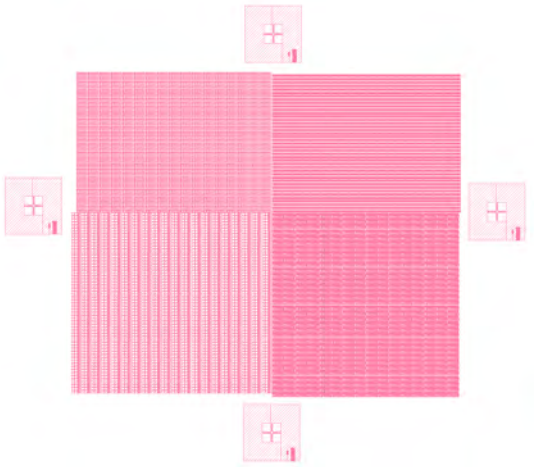

Fig. 8. Full photomask design used in fabrication of microelectrode arrays. Shaded pink areas represent the Ti-Pt bilayer.

photomask design with the square electrodes used in this paper shown in the bottom left quadrant.

Acknowledgment

The authors would like to acknowledge the support of the National Science Foundation, through NSF REU grant no. 1950720. J.Z.W. would also like to thank Zach Szekeres for his partnership, Lucas Hanson for the microfabrication tool trainings and his mentorship, and David Gonzalez-Medrano for designing and making the photomask used in the fabrication of the electrodes tested in this paper.

References

[1] Yang Bai et al. "Sensing capacitance of underwater objects in bio-inspired electrosense". In: *IEEE International Conference on Intelligent Robots and Systems*. 2012, pp. 1467–1472. ISBN: 9781467317375. DOI: 10.1109/IROS.2012.6386174.

[2] Ada-Ioana Bunea et al. "Light-Powered Microrobots: Challenges and Opportunities for Hard and Soft Responsive Microswimmers". In: *Advanced Intelligent Systems* 3.4 (Apr. 2021), p. 2000256. ISSN: 2640-4567. DOI: 10.1002/AISY.202000256. URL: https://onlinelibrary.wiley.com/doi/full/10.1002/aisy.202000256%20https://onlinelibrary.wiley.com/doi/abs/10.1002/aisy.202000256%20https://onlinelibrary.wiley.com/doi/10.1002/aisy.202000256.

[3] Hakan Ceylan et al. *Mobile microrobots for bioengineering applications*. May 2017. DOI: 10.1039/c7lc00064b. URL: https://pubs-rsc-org.ezproxy.princeton.edu/en/content/articlehtml/2017/lc/c7lc00064b%20https://pubs-rsc-org.ezproxy.princeton.edu/en/content/articlelanding/2017/lc/c7lc00064b.

[4] Alejandro Cortese et al. "CFAB: Heterogeneous Integration for Microscopic Sensors and Robots". In: *2020 CNF Annual Meeting*. 2020, p. 8. URL: https://www.cnf.cornell.edu/sites/default/files/inline-files/2020cnfAM%7B%5C_%7DProceedings.pdf.

[5] Allan H. Frey and Edwin S. Eichert. "The Nature of Electrosensing in the Fish". In: *Biophysical Journal* 12.10 (1972), pp. 1326–1358. ISSN: 00063495. DOI: 10.1016/S0006-3495(72)86166-6. URL: /pmc/articles/PMC1484230/?report=abstract%20https://www.ncbi.nlm.nih.gov/pmc/articles/PMC1484230/.

[6] Marc Z. Miskin et al. "Electronically integrated, mass-manufactured, microscopic robots". In: *Nature* 584.7822 (Aug. 2020), pp. 557–561. ISSN: 14764687. DOI: 10.1038/s41586-020-2626-9. URL: https://www.nature.com/articles/s41586-020-2626-9.

[7] James R. Solberg, Kevin M. Lynch, and Malcolm A. MacIver. "Active electrolocation for underwater target localization". In: *International Journal of Robotics Research* 27.5 (May 2008), pp. 529–548. ISSN: 02783649. DOI: 10.1177/0278364908090538. URL: http://ijr.sagepub.com.